Pergamon

Geochimica et Cosmochimica Acta, Vol. 65, No. 17, pp. 2865–2874, 2001

0016-7037/01 $20.00 + .00

PII S0016-7037(01)00626-3

Variations in Mg/Ca, Na/Ca, and Sr/Ca ratios of coral skeletons with chemical treatments: Implications for carbonate geochemistry

TAKEHIRO MITSUGUCHI,[1] TETSUO UCHIDA,[2] EIJI MATSUMOTO,[1] PETER J. ISDALE,[3] and TOSHIO KAWANA[4]

[1]Institute for Hydrospheric-Atmospheric Sciences, Nagoya University, Nagoya 464-8601, Japan
[2]Nagoya Institute of Technology, Nagoya 466-8555, Japan
[3]Australian Institute of Marine Science, P.M.B. No. 3, Townsville MC, Queensland 4810, Australia
[4]College of Education, University of the Ryukyus, Okinawa 903-0213, Japan

(*Received September* 14, 2000; *accepted in revised form March* 9, 2001)

Abstract—We made a systematic examination into the effects of chemical treatments on Mg/Ca, Na/Ca, and Sr/Ca ratios of coral skeletons. Five skeletal samples were cut from modern and fossil corals of the genus *Porites*. Each sample was ground into powder, and replicate subsamples were taken and split into four groups. One group was left untreated as the control group. The other three groups were treated cumulatively with distilled/deionized water (DDW), 30% H_2O_2, and weak HNO_3, with one group separated after each treatment step. The H_2O_2 and HNO_3 treatments incurred partial dissolution of the skeletal powder and thus resulted in considerable sample loss. All the groups were determined for the elemental ratios. The Mg/Ca and Na/Ca ratios showed decreases or little changes with the DDW treatment, and then increased with the H_2O_2 and HNO_3 treatments. The Mg/Ca and Na/Ca variations were closely parallel throughout the treatment sequence. The Sr/Ca ratio showed slight or little variation throughout the treatment sequence. These results reflect fine-scale elemental distribution in the skeletons. The Mg/Ca and Na/Ca decreases with the DDW treatment can be ascribed to removal of adsorptive Mg and Na from the skeletal surface. The Mg/Ca and Na/Ca increases with the latter treatments reflect enrichments in Mg and Na at the innermost portion of the skeletons (i.e., around the center of calcification). The Mg/Na ratio of the adsorptive phase is approximately the same as that of the skeletons. The covariation of Mg and Na in the adsorptive and skeletal phases indicates that Mg and Na behave similarly both in adsorption onto the skeletal surface and in the skeletogenesis. Sulfate ion (SO_4^{2-}) may participate in the Mg and Na behaviors. The Sr/Ca variation indicates that Sr is distributed almost homogeneously in the skeletons with little adsorptive fraction. Attention should be paid to the effects of chemical treatments associated with the fine-scale elemental heterogeneity, especially if coral Mg/Ca and Na/Ca ratios are used for paleoenvironmental analysis. *Copyright © 2001 Elsevier Science Ltd*

1. INTRODUCTION

Minor and trace elements in coral skeletons provide various proxies for paleoceanic environments. On the other hand, most of the proxies are highly affected by pre-existing contaminants (e.g., adsorptive, organic, and inorganic phases) that are disseminated throughout the skeletons. To minimize the contamination effects, the skeletons are subject to chemical treatment. Shen and Boyle (1988) established a procedure of chemical treatment for determination of trace elements (Pb, Cd, Zn, Mn, etc.) in coral skeletons, which has been widely accepted as a standard procedure (Shen and Boyle, 1987; Shen et al., 1987, 1991, 1992a,b; Lea et al., 1989; Linn et al., 1990; Shen and Sanford, 1990; Delaney et al., 1993). Compared with the trace elements, the minor elements Mg, Na, Sr, and S ranging in concentration from 500 ppm to 1% in the skeletons are less susceptible to contamination. There is no standard procedure of chemical treatment for determination of the minor elements: some researchers treat coral skeletons only with distilled water, whereas others additionally with H_2O_2 (hydrogen peroxide), NaClO (bleach), and the like for removal of organically related contamination.

The original aim of this study was to evaluate, through chemical treatments, the contamination effects on Mg/Ca, Na/Ca, and Sr/Ca ratios of coral skeletons. We unexpectedly found a side effect of chemical treatments that is associated with fine-scale elemental heterogeneity in the skeletons. Chemical treatments such as with weak acid and H_2O_2 incur dissolution of the skeletal surface. If any difference in the ratio of element A to Ca (A/Ca ratio) exists between the inner and outer parts of the skeleton, surface dissolution will cause *apparent* alteration of the bulk measurement of A/Ca ratio. We call this effect the heterogeneity effect. If the inner part has a higher A/Ca ratio than the outer part, the heterogeneity effect will appear as an increase in A/Ca ratio, whereas if the opposite happens, it will appear as a decrease in A/Ca ratio. We call the former and the latter cases positive and negative heterogeneity effects, respectively. The negative heterogeneity effect might be often mistaken for removal of contamination. Generally, the most effective means to circumvent the heterogeneity effect is to grind the skeletons into powder. However, if the skeletons have a fine-grained morphology, it is very difficult to circumvent the heterogeneity effect, because fine-scale elemental heterogeneity is prone to remain persistently in the skeletal powder. Although we ground *Porites* coral skeletons that have a fine-grained morphology (50–300 μm in thickness for main structural elements) into powder with a particle-size range of 1 to 250 μm, the positive heterogeneity effect was observed for the Mg/Ca and Na/Ca ratios. The positive heterogeneity effect for the Mg/Ca ratio is consistent with Allison (1996), who applied ion

*Author to whom correspondence should be addressed (aa153740@nyc.odn.ne.jp).

microprobe techniques to thin sections of *Porites* coral skeletons and revealed that the Mg/Ca, Sr/Ca, and Ba/Ca ratios at the innermost portion of the skeletons (i.e., around the center of calcification less than ~20 μm in width) are higher than those in the surrounding crystal area. We further found that the Mg/Ca and Na/Ca variations for the skeletal powder with chemical treatments were closely parallel, indicating that fine-scale distribution of Mg in the skeletons is similar to that of Na. Here we discuss several topics on Mg, Na, and Sr in coral skeletons: (1) adsorption onto the skeletal surface, (2) fine-scale heterogeneity in the skeletons, (3) behavior in the skeletogenesis, (4) existence mode in the skeletons, and (5) potential impact of pretreatment on Mg/Ca and Sr/Ca thermometries.

2. SAMPLES

In September 1993, a 180-cm-long core (9 cm in diameter) was hydraulically drilled from the top of a living coral colony of *Porites lutea* (~2.5 m in height) at Ishigaki Island, the Ryukyus, Japan (24°33′32″ N, 124°20′08″ E). The top of the colony was ~2.0 m in water depth (low tide).

In May 1992, a living coral colony of *Porites* sp. (~40 cm in height) was collected in Myrmidon Reef, central Great Barrier Reef (GBR), Australia (18°17′ S, 147°23′ E). The top of the colony was ~2.0 m in water depth (low tide).

In January and February 1993, core drilling was carried out through the Holocene-emerged coral reefs in the southern Okinawa Island, the Ryukyus, Japan (26°06′58″ N, 127°45′14″ E), and a 20-cm-long core (5 cm in diameter) of fossil coral (*Porites* sp.) was collected from the depth of ~5 m below mean sea level. The ^{14}C age of the fossil coral is 7210 ± 110 yr BP, which was determined by accelerate mass spectrometry at the Groningen University, the Netherlands.

The long core from Ishigaki Island was longitudinally cut into 7-mm-thick slabs by means of the equipment of the Australian Institute of Marine Science. The other specimens were cut along the growth direction into 5-mm-thick slabs with a circular rock saw. X-ray radiography for all the slabs revealed high- and low-density banding pattern. For all these specimens, high-resolution analyses of Mg/Ca and Sr/Ca ratios and $\delta^{18}O$ along the growth direction demonstrated that the high- and low-density couplet corresponds to annual band (Mitsuguchi et al., 1996, 1997; Mitsuguchi, unpublished data). More than 100 annual bands are countable in the Ishigaki specimen.

3. EXPERIMENTAL

3.1. Elemental Analysis

Three rectangular fragments were cut from 1923–1924, 1956–1957, and 1990–1991 annual bands in the Ishigaki specimen and named ISH1923, ISH1956, and ISH1990, respectively; one was cut from 1990–1991 annual bands in the GBR specimen and named GBR1990. From the Okinawa fossil specimen, a rectangular fragment containing 2 years of skeletal growth was cut and named OKIFOS. None of the fragments contained organic layers of soft tissue or symbiotic algae. The ISH1923 and ISH1990 fragments were rinsed with distilled/deionized water (DDW); the other three fragments were ultrasonically cleaned with DDW renewed repeatedly. The five fragments were then dried in a vacuum desiccator at 60°C without a drying agent, and each was ground in an acid-cleaned agate mortar. To reduce experimental uncertainty, 40 replicate subsamples weighing 6 mg each were taken from each powder sample into acid-cleaned 6-mL vials. The 40 were split into four groups, each consisting of 10 subsamples. One group was left untreated as the control group. The other three groups were treated cumulatively with DDW at room temperature, 30% H_2O_2 at 60°C, and 4 mM HNO_3 at room temperature, with one group separated after each treatment step. The procedure of the cumulative treatment is depicted in Figure 1.

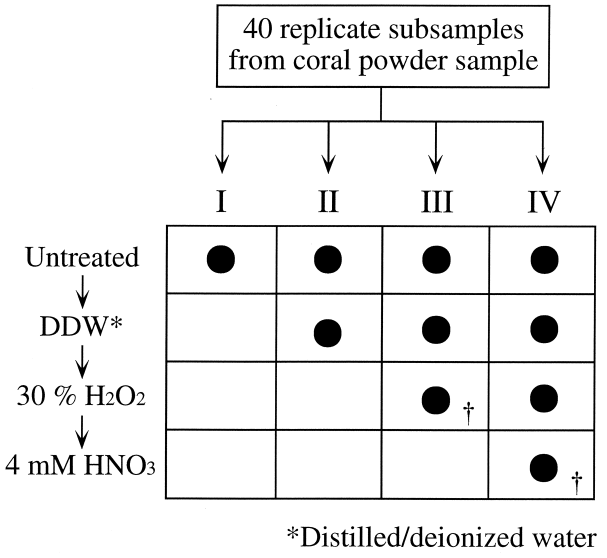

Fig. 1. Flow diagram of cumulative chemical treatment for coral powder. Forty replicate subsamples from each powder sample were split into four groups (I–IV), each consisting of 10 subsamples. For the powder sample of ISH1956, 20 supernatant liquids from the 30% H_2O_2 and 4 mM HNO_3 treatments were individually collected for measurements (†).

We designated the four groups as groups I to IV with the progress of the cumulative treatment. Each treatment was achieved with 4 mL of treatment solution per subsample and ultrasonic agitation for 15 min. At the end of each treatment, the vials were centrifuged (15 cm in radius and 2000 rpm) for 10 min, and supernatant liquid was carefully removed by siphoning with a micropipette. The treated subsamples were dried in a vacuum desiccator without a drying agent at 60°C for 12 h, and weighed again for calculation of the rates of sample loss incurred by the treatments. For ISH1956, 20 (10 + 10) supernatant liquids from the H_2O_2 and HNO_3 treatments were transferred separately into acid-cleaned 7-mL Teflon (PFA) jars (see Fig. 1) and evaporated to dryness in a clean-air-flow Teflon (TFE) chamber at 40 to 50°C for 48 h. Evaporating below 50°C prevents the H_2O_2 supernatant liquid from foaming and spattering. Thus, prepared additionally for ISH1956 were two groups of evaporated residues obtained from the H_2O_2 and HNO_3 supernatant liquids.

The prepared subsamples and evaporated residues were dissolved in 0.5 mol/L HNO_3. Calcium concentration of the sample solution was standardized to 95 ppm ± 10%. Mg, Ca, and Sr were measured by inductively coupled plasma atomic emission spectrophotometry (ICP-AES) with a Seiko SPS-7000A; Na was by acetylene-air flame atomic emission spectrophotometry (AAF-AES) with a Seiko SAS/727 atomic absorption spectrometer by use of a discrete nebulization technique (Uchida et al., 1980). Both of the instruments are equipped with a single photomultiplier. The wavelengths employed were as follows: Mg, 279.553 nm; Ca, 317.933 nm; Sr, 407.771 nm; and Na, 588.995 nm. Each element was determined in triplicate. Three and five standard solutions were prepared gravimetrically for the ICP-AES and AAF-AES measurements, respectively. Both of the instruments were calibrated with the standard solutions at intervals of six samples. Calibration curves were calculated by averaging the two calibrations bracketing the six samples, with a linear fit for ICP-AES and a parabolic fit for AAF-AES. These analytical conditions are exactly the same as those used by Mitsuguchi et al. (1996, 1997).

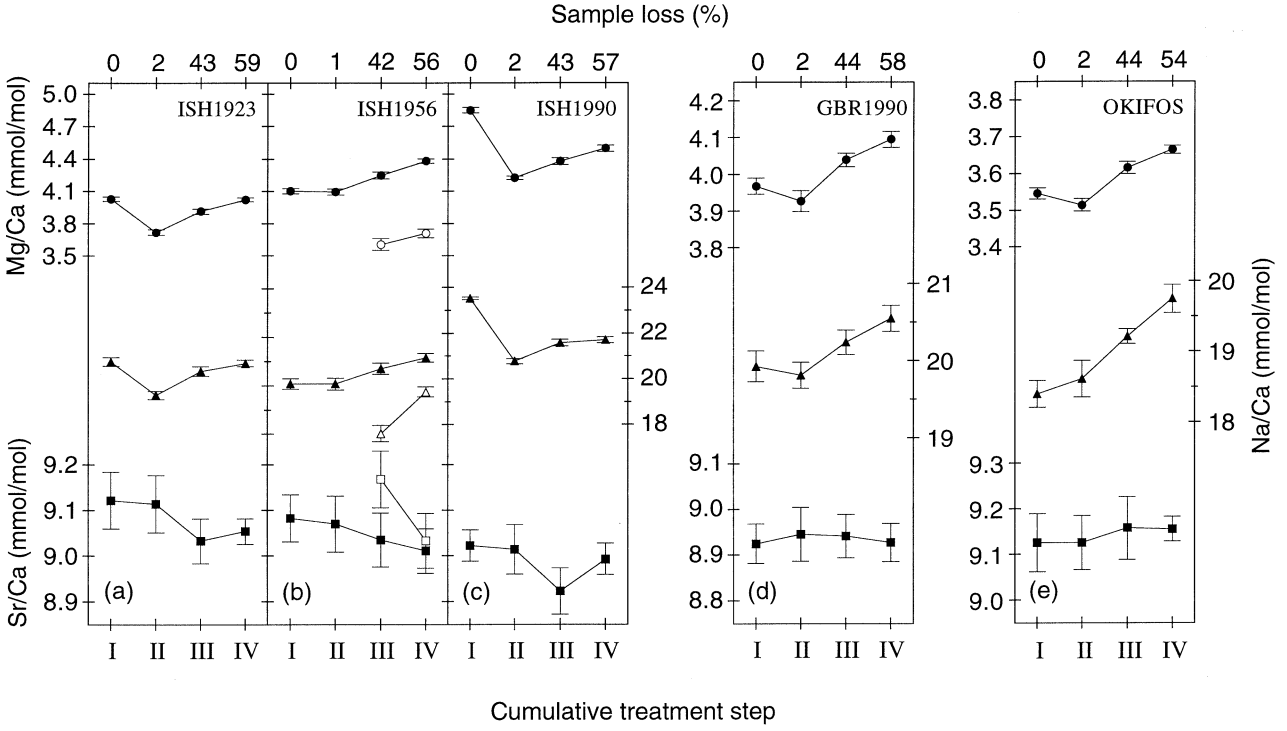

Fig. 2. Variations in Mg/Ca, Na/Ca, and Sr/Ca ratios with cumulative chemical treatment for *Porites* coral powder taken from (a) 1923–1924, (b) 1956–1957, and (c) 1990–1991 annual bands in a specimen from Ishigaki Island, (d) 1990–1991 annual bands in a specimen from the Great Barrier Reef, and (e) a 2-year increment of annual banding in a fossil specimen (7210 ± 110 yr BP) from Okinawa Island (solid symbols). The cumulative treatment steps (I–IV) are depicted in Figure 1. For the powder sample (b), supernatant liquids from steps III and IV were also determined for the elemental ratios (open symbols) (see Fig. 1). Each point is the mean value of 10 replicate subsamples with 95% confidence interval based on Student's *t* distribution. The upper axis exhibits the rate of sample loss, reflecting dissolution and siphoning losses with the cumulative treatment.

3.2. Particle-Size Analysis

Particle-size distributions of the five powder samples (untreated) were measured by laser diffraction and scattering method with a Shimadzu SALD-3000J. Typically, 72 mg of each powder sample was dispersed into 300 mL of DDW with 10-min ultrasonic agitation, then measured in quintuplicate. Dispersants such as sodium hexametaphosphate were not used because most of them incur partial dissolution of carbonate powder. The optimum refractive index for coral powder was determined in a preliminary experiment with the instrument itself. The optimum index was used consistently for all the measurements. For ISH1956, we investigated the variation in particle-size distribution with the cumulative treatment. Three groups, each consisting of triplicate subsamples, were taken from ISH1956 and treated cumulatively with the same procedure and the same quantitative ratio of subsample to treatment solution as adopted in the treatment for elemental analysis (see Fig. 1). Subsample size was adjusted beforehand so that ~24 mg each would be finally obtained after the cumulative treatment. This adjustment was based on the rates of sample loss observed in the treatment for elemental analysis. As a result, ~72 mg of treated powder was successfully obtained for each group by putting the treated subsamples together (~24 mg × 3 = ~72 mg), and measured in quintuplicate. The rate of sample loss for each group was calculated by means of the triplicate subsamples.

4. RESULTS

4.1. Elemental Analysis

Because replicate subsamples were measured in the elemental analysis, all of the results are reported as mean value with 95% confidence interval based on Student's *t* distribution. Results of the Mg/Ca, Na/Ca, and Sr/Ca ratios for all the powder samples are plotted in Figure 2 and summarized in Table 1. Considerable sample loss (~40%) is incurred by the H_2O_2 treatment because 30% H_2O_2 with a pH of ~4.2 causes partial dissolution of biogenic carbonate (Gaffey and Bronnimann, 1993; Boiseau and Juillet-Leclerc, 1997). Siphoning loss can be estimated to be <1 to 2% from the loss with the DDW treatment, which is insignificant compared with the dissolution losses with the latter treatments. Results of the supernatant liquids from the treatments for ISH1956 are shown in Figure 2b and listed in Table 2. By use of Tables 1b and 2 it is confirmed that mass balances of elements before and after the treatments are almost equal (<2.5% discrepancies).

For all the powder samples, the Mg/Ca and Na/Ca ratios showed decreases or little changes with the DDW treatment, and then increased with the H_2O_2 and HNO_3 treatments. The Mg/Ca and Na/Ca variations closely mimic each other throughout the treatment sequence. The Mg/Ca and Na/Ca decrements with the DDW treatment for ISH1923 and ISH1990 (7–13%; Figs. 2a,c) are conspicuously larger than those for the other samples (<1.5%; Figs. 2b,d,e). Before grinding the skeletal fragments, ISH1923 and ISH1990 were only rinsed with DDW, whereas the other fragments were ultrasonically cleaned with DDW renewed repeatedly. Figure 3 presents a plot of Mg/Ca

Table 1. Summary of variations in Mg/Ca, Na/Ca, and Sr/Ca ratios with cumulative chemical treatment for *Porites* coral powder taken from (a) 1923–1924, (b) 1956–1957, and (c) 1990–1991 annual bands in a specimen from Ishigaki Island, (d) 1990–1991 annual bands in a specimen from the Great Barrier Reef, and (e) 2-year increment of annual banding in a fossil specimen (7210 ± 110 yr BP) from Okinawa Island.

Chemical treatment[a]	Sample loss[b] (%)	Mg/Ca[c] (mmol/mol)	Na/Ca[c] (mmol/mol)	Sr/Ca[c] (mmol/mol)
(a) ISH1923				
Untreated	0	4.03 ± 0.02	21.0 ± 0.2	9.12 ± 0.06
+ DDW[d]	1.7	3.72 ± 0.03	19.6 ± 0.2	9.11 ± 0.06
+ 30% H_2O_2	42.5	3.91 ± 0.02	20.6 ± 0.2	9.03 ± 0.05
+ 4 mM HNO_3	59.0	4.02 ± 0.02	20.9 ± 0.1	9.05 ± 0.03
(b) ISH1956				
Untreated	0	4.10 ± 0.02	19.8 ± 0.2	9.08 ± 0.05
+ DDW	1.2	4.09 ± 0.03	19.8 ± 0.3	9.07 ± 0.06
+ 30% H_2O_2	41.5	4.25 ± 0.03	20.5 ± 0.2	9.03 ± 0.06
+ 4 mM HNO_3	56.2	4.38 ± 0.02	20.9 ± 0.2	9.01 ± 0.05
(c) ISH1990				
Untreated	0	4.85 ± 0.03	23.5 ± 0.1	9.02 ± 0.03
+ DDW	1.9	4.22 ± 0.02	20.8 ± 0.1	9.01 ± 0.05
+ 30% H_2O_2	43.2	4.38 ± 0.03	21.6 ± 0.1	8.92 ± 0.05
+ 4 mM HNO_3	57.0	4.50 ± 0.03	21.7 ± 0.1	8.99 ± 0.03
(d) GBR1990				
Untreated	0	3.97 ± 0.02	19.9 ± 0.2	8.93 ± 0.04
+ DDW	2.3	3.93 ± 0.03	19.8 ± 0.2	8.95 ± 0.06
+ 30% H_2O_2	44.0	4.04 ± 0.02	20.2 ± 0.2	8.94 ± 0.05
+ 4 mM HNO_3	57.5	4.10 ± 0.02	20.5 ± 0.2	8.93 ± 0.04
(e) OKIFOS (^{14}C age of 7210 ± 110 yr BP)				
Untreated	0	3.55 ± 0.02	18.4 ± 0.2	9.13 ± 0.06
+ DDW	2.5	3.51 ± 0.02	18.6 ± 0.3	9.13 ± 0.06
+ 30% H_2O_2	44.4	3.62 ± 0.02	19.2 ± 0.1	9.16 ± 0.07
+ 4 mM HNO_3	53.8	3.67 ± 0.01	19.8 ± 0.2	9.16 ± 0.03

[a] Procedure of the chemical treatment is depicted in Figure 1.
[b] Results are given as mean value of 10 replicate subsamples.
[c] Results are given as mean value of 10 replicate subsamples with 95% confidence interval based on Student's *t* distribution (mean ± t s/$\sqrt{n}$; n = 10, t = 2.262, s = standard deviation).
[d] Distilled/deionized water.

vs. Na/Ca ratios for the results of all the powder samples shown in Figure 2. In the Mg/Ca-Na/Ca plot, all the samples exhibit similar slopes for the variation with the cumulative treatment, which are subparallel to the line:

$$\text{Mg/Ca (mmol/mol)} = 0.2 \times \text{Na/Ca (mmol/mol)}.$$

Furthermore, all the samples are plotted close to the line. Consequently, Mg/Na ratios of all the samples show little variation throughout the treatment sequence, converging around 0.2 mol/mol. Results for the Sr/Ca ratio seem a little inconsistent. For ISH1923, ISH1956, and ISH1990 that are from the same specimen, the Sr/Ca ratios appear to decrease slightly with the H_2O_2 treatment (Figs. 2a–c); whereas for GBR1990 and OKIFOS, there is no evidence of change throughout the treatment sequence (Figs. 2d,e). For ISH1956, significant Sr/Ca difference can be seen between the H_2O_2-treated powder and its supernatant liquid (Fig. 2b).

Table 2. Mg/Ca, Na/Ca, and Sr/Ca ratios of supernatant liquids from the 30% H_2O_2 and 4 mM HNO_3 treatments for ISH1956.

Supernatant liquid[a]	Mg/Ca[b] (mmol/mol)	Na/Ca[b] (mmol/mol)	Sr/Ca[b] (mmol/mol)
30% H_2O_2	3.61 ± 0.05	17.6 ± 0.3	9.17 ± 0.06
4 mM HNO_3	3.71 ± 0.04	19.4 ± 0.2	9.03 ± 0.06

[a] Ten supernatant liquids were separately collected from each treatment (see Fig. 1).
[b] Results are given as mean value of 10 evaporated residues with 95% confidence interval based on Student's *t* distribution (mean ± t s/$\sqrt{n}$; n = 10, t = 2.262, s = standard deviation).

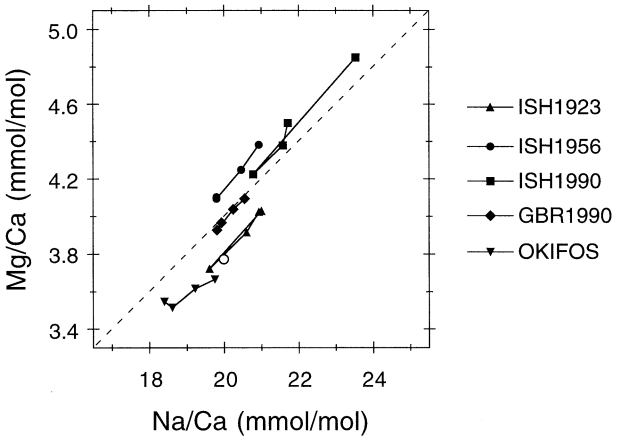

Fig. 3. Plot of Mg/Ca vs. Na/Ca ratios derived from the data presented in Figure 2 and Table 1. The open circle represents additional data point obtained from another fossil *Porites* coral (see "Discussion"). Horizontal and vertical errors (95% confidence intervals) for each point are as small as the symbol size. Note that all the samples exhibit similar slopes for the variation with the cumulative treatment, which are subparallel to the dashed line: Mg/Ca (mmol/mol) = 0.2 × Na/Ca (mmol/mol). Furthermore, all the points are plotted close to the line.

4.2. Particle-Size Analysis

All the powder samples (untreated) showed similar particle-size distributions ranging from ~1 to ~250 μm with a peak at ~100 μm. Variation in the particle-size distribution for ISH1956 with the cumulative treatment is shown in Figure 4. Fine particles (<~20 μm) were dissolved with the H_2O_2 treatment, and thus, the percentage of coarse particles (80–200 μm) was increased. The rates of sample loss were almost the same as that observed in the treatment for the elemental analysis.

5. DISCUSSION

The Mg/Ca and Na/Ca decreases with the DDW treatment are consistent with results reported by Amiel et al. (1973) and Yoshioka et al. (1985). Amiel et al. (1973) immersed coral skeletons in distilled water for 140 d with renewal of the water each day and observed rapid and preferential release of Mg, Na, and K from the skeletons in the initial 20 d. They concluded that Mg, Na, and K are partly (10–30% of each total) adsorbed on the skeletal surface. Yoshioka et al. (1985) immersed *Porites* coral skeletons in NaCl aqueous solution for >50 d with renewal of the solution every several days and observed the same phenomenon for Mg. Adsorptive or exchangeable Mg was reported also for abiogenic aragonite and biogenic calcite (Walls et al., 1977; Love and Woronow, 1991). Allison (1996) demonstrated higher concentrations of Mg and Ba on the sur-

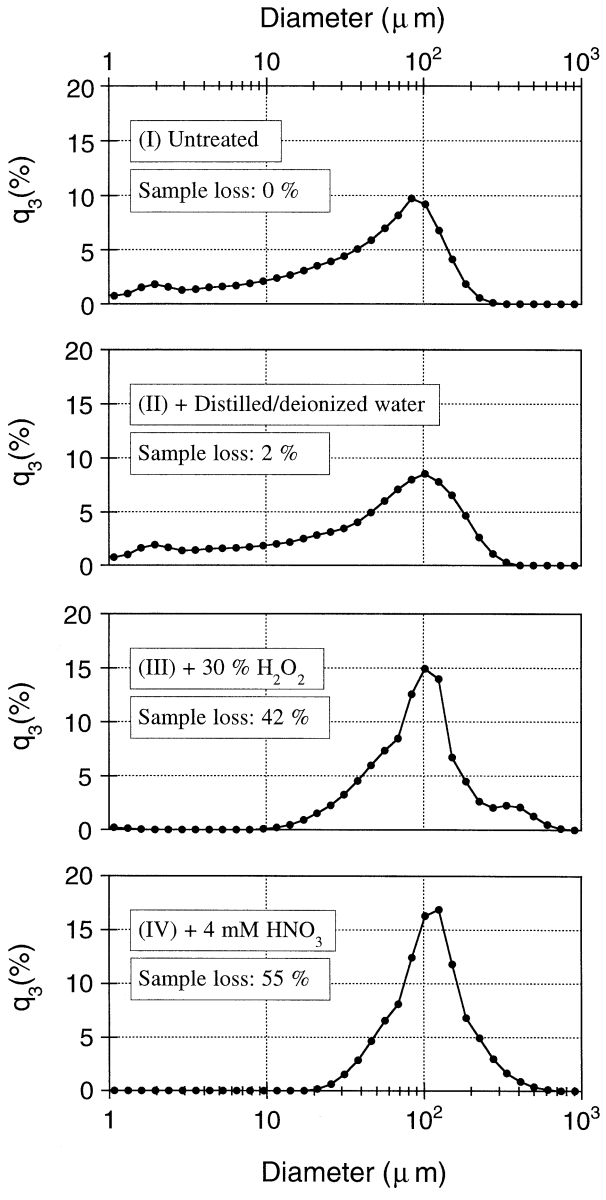

Fig. 4. Variation in particle-size distribution of *Porites* coral powder with the cumulative treatment steps: (I) untreated, (II) DDW, (III) 30% H_2O_2, and (IV) 4 mM HNO_3, which are depicted in Figure 1. The q_3 (%) represents volume fraction of the particle. Note that fine particles (less than ~20 μm) disappear and the percentage of coarse particles (80–200 μm) increases with steps III and IV, which incur partial dissolution of coral powder.

face of *Porites* coral skeletons by ion microprobe analysis and ascribed the observations to ionic adsorption from seawater. Taken together, our results indicate that coral skeletal surface is enriched in adsorptive Mg and Na from seawater. The larger decreases (7–13%) in the Mg/Ca and Na/Ca ratios for ISH1923 and ISH1990 indicate that the treatment before grinding these samples was not sufficient to remove adsorptive Mg and Na (see sections 3.1 and 4.1).

The Mg/Ca and Na/Ca increases with the H_2O_2 and HNO_3 treatments are unexpected because the matrix of coral skeletons is $CaCO_3$ and because considerable part of contamination (e.g., organic materials, inorganic precipitation) is expected to be removed with the treatments. Considering that the H_2O_2 and HNO_3 treatments incurred partial dissolution of the skeletal powder, the Mg/Ca and Na/Ca increases can be ascribed to positive heterogeneity effect (see "Introduction"). Detailed explanation for the Mg/Ca and Na/Ca increases is as follows (Fig. 5): (1) Mg and Na concentrations at the innermost portion of the skeletons (i.e., around the center of calcification) are higher than those in the surrounding area, (2) the elemental heterogeneity remains persistently even after the skeletons are ground into powder, (3) adsorptive Mg and Na are removed from the skeletal surface with the DDW treatment, and (4) partial dissolution of the skeletal powder with the H_2O_2 and HNO_3 treatments causes *apparent* increases of the Mg/Ca and Na/Ca ratios in bulk measurement.

This explanation is given in the light of the findings of Allison (1996), who found that the Mg/Ca, Sr/Ca, and Ba/Ca ratios at the innermost portion of *Porites* coral skeletons (i.e., around the center of calcification less than ~20 μm in width) are higher than those in the surrounding crystal area. Sinclair et al. (1998) and Fallon et al. (1999) also observed fine-scale heterogeneity of Mg in *Porites* coral skeletons by laser ablation—inductively coupled plasma mass spectrometry (LA-ICP-MS). Because *Porites* corals have a fine-grained skeletal morphology (50–300 μm in thickness for main structural elements), the innermost portion of the skeletons is finely reticulated throughout the morphology. We ground the skeletons into powder with a particle-size range of 1 to 250 μm before the cumulative treatment. However, the innermost skeletal portion (less than ~20 μm in width) still remains inside the coarse particles. The H_2O_2 treatment causes surface dissolution of the coarse particles as well as complete dissolution of the fine particles (less than ~20 μm), and the following HNO_3 treatment promotes surface dissolution of the coarse particles (Fig. 4), leaving the innermost skeletal portion selectively. Thus, we conclude that the Mg/Ca and Na/Ca increases are due to the fine-scale heterogeneity of Mg and Na, as described in Figure 5. Because the skeletal dissepiments of *Porites* corals are as thin as ~10 μm (Le Tissier et al., 1994), they have little contribution to our data. The heterogeneity effect probably varies in degree among coral genera because it should be dependent on skeletal morphology. For example, because a massive coral genus, *Montastrea*, has a relatively coarse skeletal morphology, the heterogeneity effect may be more easily circumvented by grinding the skeletons.

Applying the above discussion to the Sr/Ca results, the following views can be obtained: the amount of adsorptive Sr is negligible compared with that of skeletally incorporated Sr, and fine-scale distribution of Sr in the skeletons is almost homogeneous. These views are in accord with the suggestion of Amiel et al. (1973). The slight Sr/Ca decrease (<1%) with the H_2O_2 treatment for ISH1923, ISH1956, and ISH1990 may represent negative heterogeneity effect (see "Introduction"): the inner part of the skeletons may have slightly lower Sr concentration than the outer part. Allison (1996), however, reported that the innermost skeletal portion has a little higher Sr/Ca ratio (up to 6%) than the surrounding area. We refrain from discussing the discrepancy because the Sr/Ca decrease we observed is indistinct. In Allison (1996), the Mg/Ca difference between the innermost skeletal portion and the surrounding

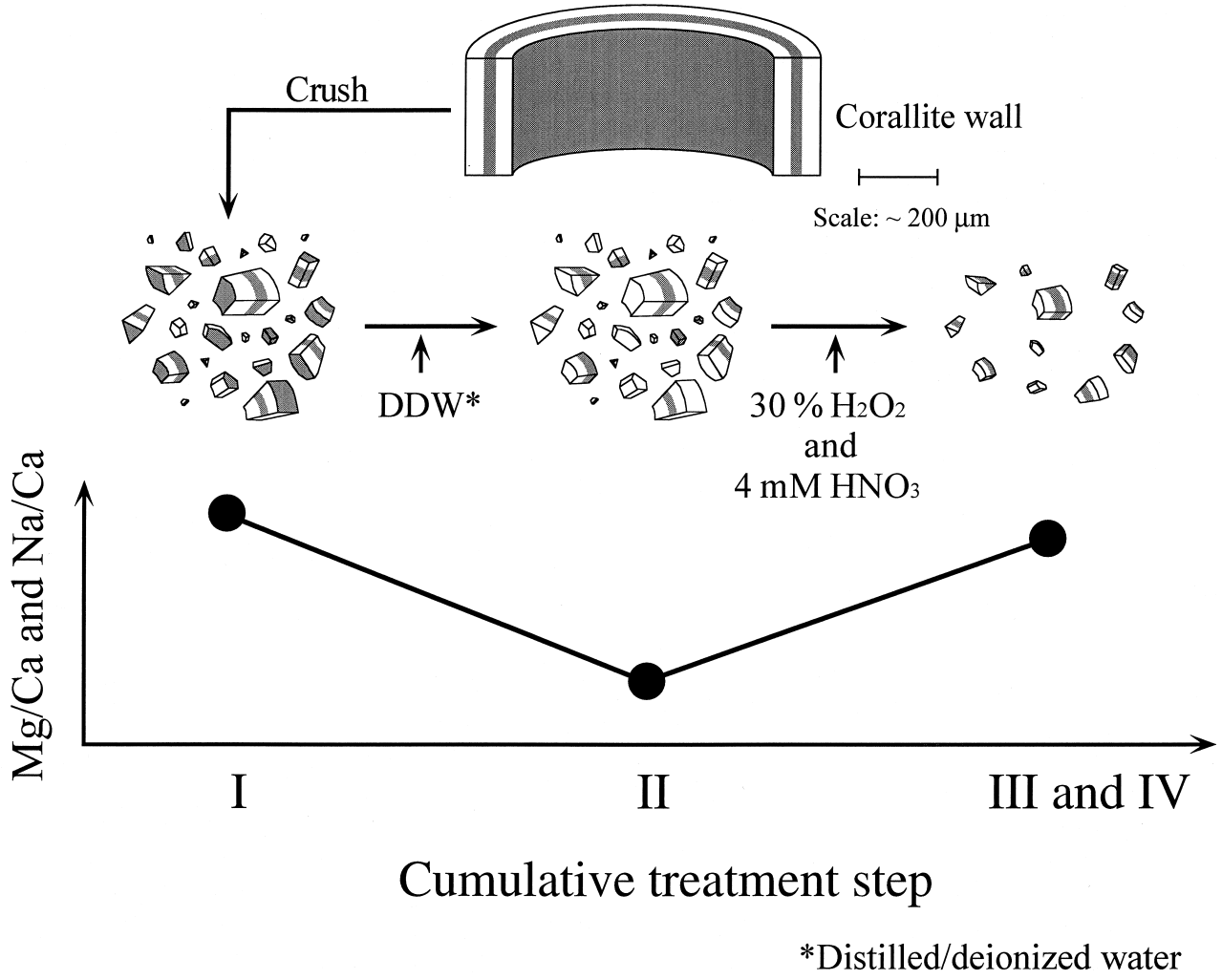

Fig. 5. Schematic illustration of fine-scale distributions of Mg and Na in *Porites* coral skeletons and the effects of cumulative chemical treatment on bulk measurements of the Mg/Ca and Na/Ca ratios for the powder sample. The skeletal surface and the innermost portion of the skeletons (i.e., around the center of calcification less than ~20 μm in width) are enriched in Mg and Na (shaded areas). The innermost skeletal portion is exaggeratedly described. The cumulative treatment steps (I–IV) are depicted in Figure 1.

area is much larger (up to 40%). Thus, it is likely that such a strong heterogeneity in the Mg/Ca ratio appears in our bulk analysis, whereas such a weak heterogeneity in the Sr/Ca ratio does not. The fossil sample, OKIFOS, showed the same results as seen in the other modern samples, implying that the elemental heterogeneity is well preserved.

The strong covariation of Mg and Na in the adsorptive and skeletal phases indicates that Mg and Na behave similarly both in adsorption onto the skeletal surface and in the skeletogenesis. The Mg/Na ratio of the adsorptive phase can be estimated to be 0.22 to 0.23 mol/mol from the ISH1923 and ISH1990 data (Table 1), and that of the skeletal phase is 0.18 to 0.21 mol/mol (Fig. 3). In Figure 3, we present additional Mg/Ca-Na/Ca data obtained from another fossil *Porites* coral (6750 ± 45 yr BP) from southern Okinawa Island, the Ryukyus, Japan (T. Mitsuguchi, unpublished data), which gives a skeletal Mg/Na ratio of ~0.19 mol/mol. Thus, the Mg/Na ratios in the processes of adsorption and skeletogenesis are restricted to ~0.2 mol/mol. Our results accord well with those of Bar-Matthews et al. (1993), who applied electron probe microanalysis to modern and fossil corals (*Montastrea annularis* and *Acropora palmata*) and found positive correlations of Mg, Na, and S for various types of aragonite: "main coral matrix," "fibers in fibrous micropore," and "projecting needle." The latter two types consist of secondary aragonite that is diagenetically precipitated in the skeletons.

By use of the data shown in Bar-Matthews et al. (1993), we calculated Mg/Na and Na/S ratios for each type (Table 3). Mg/Na ratio of the main coral matrix is 0.200 ± 0.028 mol/mol, which agrees well with our results. All the types show the same Na/S ratio of ~3.2 mol/mol, indicating that Na and S behave similarly through various processes (e.g., skeletogenesis, recrystallization, diagenesis). Although Bar-Matthews et al. (1993) gave the Na/S ratio as ~0.25 mol/mol, this is a miscalculation. Enmar et al. (2000) confirmed the Mg-Na-S correlations for *Porites* sp. and reported that Ca concentrations

Table 3. Mg/Na and Na/S ratios for three types of aragonite in coral skeletons calculated using the data shown in Bar-Matthews et al. (1993).

Type of aragonite	Mg/Na (mol/mol)[a]	Na/S (mol/mol)[a]
Main coral matrix[b]	0.200 ± 0.028	3.19 ± 0.19
Fibers in fibrous micropore[c]	0.172 ± 0.032	3.19 ± 0.34
Projecting needle[c]	0.122 ± 0.084	3.19 ± 0.69

[a] Calculation represents mean value with standard deviation.
[b] Samples containing calcite or oolite are excluded.
[c] Secondary aragonite.

in main coral matrix and secondary aragonite are almost equal (388,000–389,000 ppm). We compared our Mg/Ca-Na/Ca plot (Fig. 3) with the plot obtained by combination of Bar-Matthews et al. (1993) and Enmar et al. (2000) (Fig. 6a). Our Mg/Ca-Na/Ca data lie just in the area of main coral matrix. The S/Ca-Na/Ca plot obtained by combination of Bar-Matthews et al. (1993) and Enmar et al. (2000) is also shown in Figure 6b.

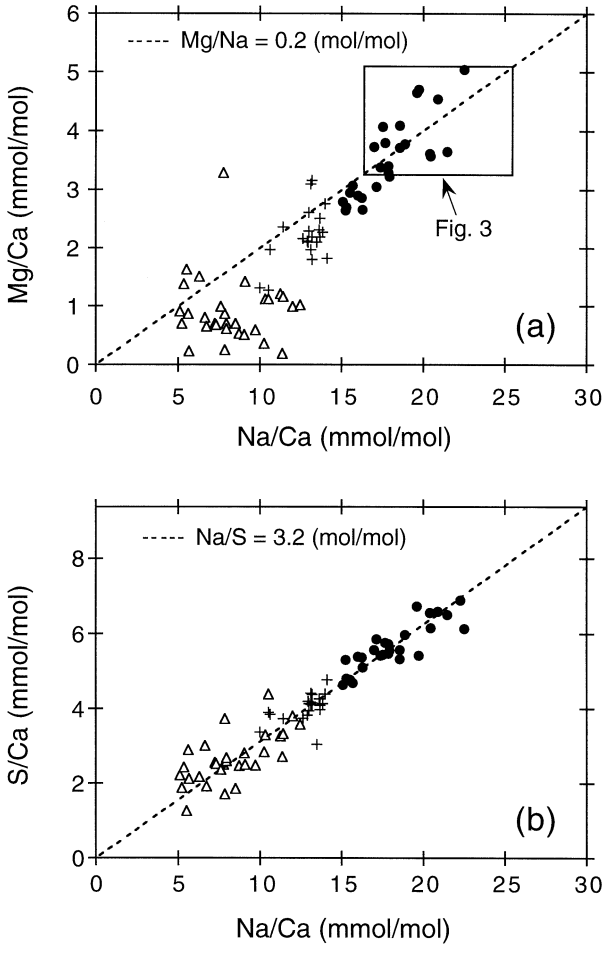

Fig. 6. (a) Comparison between the Mg/Ca-Na/Ca plot obtained in this study (Fig. 3) and the plot obtained by combination of Bar-Matthews et al. (1993) and Enmar et al. (2000). (b) The S/Ca-Na/Ca plot obtained by combination of Bar-Matthews et al. (1993) and Enmar et al. (2000). Symbols are as follows: filled circle, cross, and open triangle represent the main coral matrix, fibers in fibrous micropore, and projecting needle, respectively. The Mg/Na and Na/S ratios for each material are statistically listed in Table 3. Note that our Mg/Ca-Na/Ca plot (Fig. 3) lies just in the area of the main coral matrix.

Combined, we propose a general trend that Mg, Na, and S behave similarly with an approximate molar ratio of Mg:Na:S = 16:80:25 in the processes of adsorption, skeletogenesis, and diagenetic precipitation, although Mg behavior in the diagenetic process seems to deviate a little from this trend (see Fig. 6a and Table 3). Needless to say, the elemental molar ratio is variable to a certain degree because environmental controls on these elements are different, which will be discussed later. The elemental molar ratio is quite different from that in seawater of Mg:Na:S = 47:415:25. Although we cannot give persuasive explanation for the difference, we infer that the correlative behaviors of Mg, Na, and S are related to the affinity of SO_4^{2-} for Mg^{2+} and Na^+ in seawater. In seawater, S exists as SO_4^{2-}, partly forming ion pairs with Mg, Na, and Ca (40–50% for SO_4^{2-}, 15–25% for $MgSO_4^0$, 20–40% for $NaSO_4^-$, and ~5% for $CaSO_4^0$) (Dyrssen and Wedborg, 1974; Garrels and Thompson, 1962; Kester and Pytkowicz, 1968, 1969; Pytkowicz and Hawley, 1974). Thus, it is likely that Mg and Na behave partly as ion pairs with SO_4^{2-} in the processes of adsorption and skeletogenesis; consequently, the skeletal surface and the innermost skeletal portion may be enriched also in SO_4^{2-}.

Correlative behaviors of Na^+ and SO_4^{2-} have also been observed in carbonate coprecipitation experiments (Kitano et al., 1975; Busenberg and Plummer, 1985). It comes into question whether $MgSO_4^0$ and $NaSO_4^-$ can be incorporated into aragonite lattice. Various complex species (e.g., $UO_2CO_3^0$, $UO_2(CO_3)_2^{2-}$, HBO_3^-) are believed to exist in coral aragonite lattice (Swart and Hubbard, 1982; Vengosh et al., 1991; Hemming and Hanson, 1992; Gaillardet and Allègre, 1995; Min et al., 1995; Shen and Dunbar, 1995), although considerable distortion of the crystal lattice would be involved. Therefore, no reason exists to deny that $MgSO_4^0$ and $NaSO_4^-$ are incorporated into the lattice. By X-ray absorption spectroscopy, Pingitore et al. (1995) indicated that S is present as SO_4^{2-} in coral aragonite, although it remains uncertain whether SO_4^{2-} replaces CO_3^{2-}. Likewise, the locations for Mg and Na in aragonite lattice remain uncertain in spite of much attention by many researchers. From a crystallographic viewpoint, Mg^{2+} does not fit into the nine-fold orthorhombic aragonite coordination (i.e., CaO_9 polyhedron) because of its smaller ionic radius compared with Ca^{2+} (Shannon, 1976). The system $CaCO_3$-$MgCO_3$ is isostructural with calcite, which has a tighter rhombohedral structure (CaO_6 octahedron). Therefore, it has been suggested that Mg^{2+} may be loosely bound to aragonite lattice (Amiel et al., 1973; Mitsuguchi et al., 1996). Although Na^+ is comparable in size to Ca^{2+}, there is a question how the charge balance of aragonite is maintained if it does substitute for Ca^{2+}. Land and Hoops (1973) suggested that Na^+ together with HCO_3^- may be incorporated into marine carbonates. On the other hand, it has been strongly suggested, for both calcite and aragonite, that interstitial locations are available for monovalent cations such as Na^+ and K^+ (White, 1977; Ishikawa and Ichikuni, 1984; Busenberg and Plummer, 1985). Busenberg and Plummer (1985) synthesized calcite and suggested that a larger amount of Na^+ is incorporated into crystal defects or distortions (i.e., expanded interstitial spaces). Considering these crystallographic suggestions, the incorporations of $MgSO_4^0$ and $NaSO_4^-$ into aragonite lattice would expand the

surrounding interstitial spaces, into which additional Mg^{2+} and Na^{+} might be incorporated. The enrichments in Mg and Na at the innermost skeletal portion may be due to higher density of crystal defects produced by very rapid crystal growth at the center of calcification, into which larger amounts of $MgSO_4^0$, $NaSO_4^-$, Mg^{2+}, and Na^{+} are possibly incorporated. Allison (1996) and Wainwright (1964) observed lower density of carbonate material around the center of calcification, which may represent higher density of crystal defects. Thus, in coral aragonite, Mg and Na may exist partly as interstitial ions associated with SO_4^{2-}, possibly coinciding with crystal defects or distortions.

A variety of minor and trace elements in biogenic carbonates are frequently associated with organic phase in the matrix, which sometimes becomes a crucial problem in carbonate geochemistry. The effect of organic phase varies in degree from element to element. Thus, we discuss this subject for Mg, Na, and Sr in coral skeletons. Hart et al. (1997) reported typical organic-carbon content of *Porites* coral skeletons as 0.4 to 0.7 wt% for the skeletal part, containing no organic layers of soft tissue or symbiotic algae. They also demonstrated that ~75% of the organic carbon can be removed with chemical treatments, whereas the remaining organic carbon is well sequestered in the skeletal matrix. A brief outline of their treatment method is as follows: grinding the skeletons (*Porites* sp.) into powder with a particle size of <300 μm; and cumulatively treating the powder with 3 and 10% H_2O_2 (unbuffered), weak HNO_3, and 5% NaClO (this proved to be ineffective), which is very similar to our method. Thus, our treatment method probably removes a considerable part of the skeletally bound organic materials, as observed in Hart et al. (1997). If Mg, Na, and Sr in the skeletons are significantly associated with organic materials, it is expected that the concentrations of these elements in the skeletons decrease with the H_2O_2 and HNO_3 treatments.

Unexpectedly, as shown in Figure 2, the Mg/Ca and Na/Ca ratios increased with these treatments, which can be ascribed to positive heterogeneity effect (see above discussion), whereas the Sr/Ca ratio showed little change. Therefore, we suggest that Mg, Na, and Sr in *Porites* coral skeletons are not significantly associated with organic materials. However, considering that part of the organic materials probably remain in the skeletons after the H_2O_2 and HNO_3 treatments, and considering that these treatments incurred partial dissolution of the skeletal powder (i.e., heterogeneity effect), our suggestion may need further examination. On the other hand, Figures 3 and 6a,b seem to support our suggestion because they demonstrate that the ratio of Mg:Na:S in the main coral matrix is close to the ratio in the secondary aragonite or in the adsorptive phase, implying that the incorporations of these elements into coral skeletons are controlled only by inorganic processes. Delaney et al. (1996) showed no changes in the Mg/Ca and Sr/Ca ratios of *Halimeda* algal aragonite with NaOH-buffered H_2O_2 treatment and also reported similar results for the Mg/Ca and Sr/Ca ratios of *Porites* coral skeletons, which is compatible with our suggestion. Although Amiel et al. (1973) suggested that Mg, Na, Sr, and K in coral skeletons are significantly associated with organic materials, their experimental method for this particular observation seems very rough.

Cyclical variation of Mg/Ca ratio along the growth axis of coral skeletons was reported first by Goreau (1977) and Oomori et al. (1982). Mitsuguchi et al. (1996) showed that the cyclical Mg/Ca variation represents seasonal variation of seawater temperature. Although coral Na/Ca and S/Ca ratios show similar variations along the skeletal growth axis, they have no temperature-induced signals (Oomori et al., 1982; Mitsuguchi, unpublished data). Environmental controls for coral Na/Ca and S/Ca ratios are poorly understood. To sum up, although there is a general trend that Mg, Na, and S behave similarly in coral skeletogenesis, only the Mg/Ca ratio is evidently controlled by temperature. In any case, the positive heterogeneity effect on the Mg/Ca and Na/Ca ratios should be taken into consideration if they are used for paleoenvironmental analysis. The Mg/Ca–temperature relationship given in Mitsuguchi et al. (1996) is probably affected by the positive heterogeneity effect because they used the same specimen that we did in this study (the Ishigaki specimen) and treated the subsamples cumulatively with DDW, 4 mM HNO_3, and 30% H_2O_2 (at 60°C), in that order. For ISH1923, ISH1956, and ISH1990, which are from the Ishigaki specimen, the Mg/Ca increments through the H_2O_2 and HNO_3 treatments are consistently ~0.3 mmol/mol (see Table 1 and Fig. 2). Thus, positive heterogeneity effect on the Mitsuguchi et al. (1996) relationship is probably ~0.3 mmol/mol. Two Mg/Ca–temperature relationships for *Porites* corals have been calibrated by LA-ICP-MS with skeletal samples treated only with ultrapure water (Sinclair et al., 1998; Fallon et al., 1999). Compared with the two relationships, the Mitsuguchi et al. (1996) relationship gives higher Mg/Ca ratio in the calibrated temperature range (Fig. 7). Subtracting the positive heterogeneity effect of ~0.3 mmol/mol makes the Mitsuguchi et al. (1996) relationship approach and overlap the Sinclair et al. (1998) relationship.

The dependence of coral Sr/Ca ratio on temperature was suggested by Weber (1973), confirmed by Smith et al. (1979) and Schneider and Smith (1982), and developed by Beck et al. (1992) for practical use as a paleothermometer. Thereafter, the Sr/Ca thermometry has been widely used for reconstruction of paleoceanic climate in tropical regions (Guilderson et al., 1994; McCulloch et al., 1996, 1999; Beck et al., 1997; Gagan et al., 1998). The slight or little variation ($<1\%$) of coral Sr/Ca ratio with chemical treatments seems to enhance the usefulness of the Sr/Ca thermometry. Nonetheless, attention should be paid to heterogeneity effect on the Sr/Ca thermometry because the Sr/Ca ratio has low sensitivity to temperature (~0.7%/°C).

6. SUMMARY

We investigated the variations in Mg/Ca, Na/Ca, and Sr/Ca ratios of *Porites* coral skeletons with the cumulative treatment with DDW, 30% H_2O_2, and 4 mM HNO_3, and obtained implications for fine-scale distributions of Mg, Na, and Sr in the skeletons and for behaviors of Mg and Na both in adsorption onto the skeletal surface and in the skeletogenesis. Some published works (e.g., Bar-Matthews et al., 1993; Allison, 1996) were very helpful for our extensive discussion.

The Mg/Ca and Na/Ca variations with the cumulative treatment were closely parallel: decrease with the DDW treatment, which is due to removal of adsorptive Mg and Na from the skeletal surface; then increase with the following H_2O_2 and HNO_3 treatments, which reflects enrichments in Mg and Na at

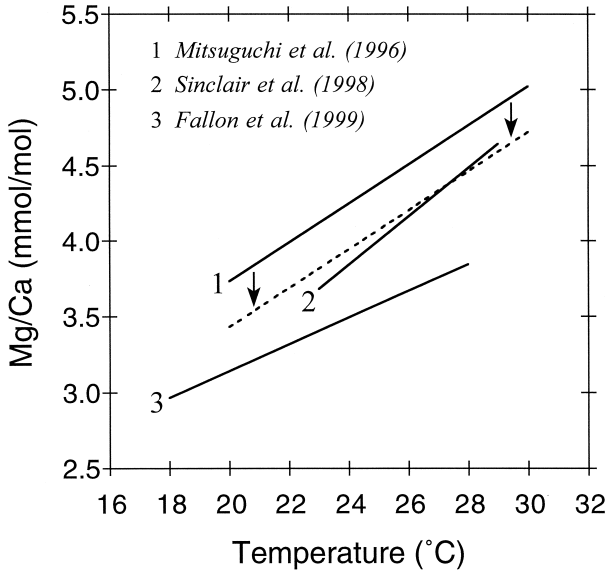

Fig. 7. Mg/Ca-temperature relationships for *Porites* coral skeletons. The Mitsuguchi et al. (1996) relationship was obtained by ICP-AES with skeletal subsamples treated cumulatively with DDW, 4 mM HNO_3, and 30% H_2O_2 in that order, whereas the Sinclair et al. (1998) and Fallon et al. (1999) relationships were obtained by LA-ICP-MS with skeletal samples treated only with ultrapure water. The HNO_3 and H_2O_2 treatments probably caused a positive heterogeneity effect on the Mitsuguchi et al. (1996) relationship. As described by dashed line, subtracting the positive heterogeneity effect makes the Mitsuguchi et al. (1996) relationship approach and overlap the Sinclair et al. (1998) relationship.

the innermost portion of the skeletons (i.e., around the center of calcification less than ~20 μm in width). Because the H_2O_2 and HNO_3 treatments dissolve the outer part of the skeletons, the innermost skeletal portion, enriched in Mg and Na, is prone to selectively remain after the treatments. Thus, the Mg/Ca and Na/Ca increases are experimental artifacts associated with the fine-scale elemental heterogeneity. We call this effect the heterogeneity effect. The Sr/Ca ratio showed slight or little variation throughout the treatment sequence, indicating that Sr is distributed almost homogeneously in the skeletons with little adsorptive fraction. Heterogeneity effect should be taken into consideration, especially if the Mg/Ca and Na/Ca ratios are used for paleoenvironmental analysis.

The remarkable covariation of Mg and Na in the adsorptive and skeletal phases indicates that Mg and Na behave similarly both in adsorption onto the skeletal surface and in the skeletogenesis. Furthermore, we found that the adsorptive and skeletal phases have similar Mg/Na ratios (0.18–0.23 mol/mol). Combined with the positive correlations of Mg, Na, and S observed for coral aragonite and secondary aragonite (Bar-Matthews et al., 1993), it can be deduced that Mg, Na, and S behave similarly in the processes of adsorption, skeletogenesis, and diagenetic precipitation. The correlative behaviors of Mg, Na, and S can be related to the fact that SO_4^{2-} forms ion pairs with Mg^{2+} and Na^+ in seawater ($MgSO_4^0$ and $NaSO_4^-$).

Acknowledgments—We thank Nicky Allison and Mira Bar-Matthews for insightful reviews and David W. Lea for constructive advice. We also thank Bruce Parker, Osamu Abe, and Hironobu Kan for collecting the modern and fossil corals, Takanori Okamoto for technical support in particle-size analysis, and Hiroyuki Kitagawa for ^{14}C determination of fossil corals. This work was supported by Grant-in-Aid for Japan Society for the Promotion of Science (JSPS) fellows (199803075).

Associate editor: D. W. Lea

REFERENCES

Allison N. (1996) Geochemical anomalies in coral skeletons and their possible implications for palaeoenvironmental analyses. *Mar. Chem.* **55,** 367–379.

Amiel A. J., Friedman G. M., and Miller D. S. (1973) Distribution and nature of incorporation of trace elements in modern aragonitic corals. *Sedimentology* **20,** 47–64.

Bar-Matthews M., Wasserburg G. J., and Chen J. H. (1993) Diagenesis of fossil coral skeletons: Correlation between trace elements, textures, and $^{234}U/^{238}U$. *Geochim. Cosmochim. Acta* **57,** 257–276.

Beck J. W., Edwards R. L., Ito E., Taylor F. W., Récy J., Rougerie F., Joannot P., and Henin C. (1992) Sea-surface temperature from coral skeletal strontium/calcium ratios. *Science* **257,** 644–647.

Beck J. W., Récy J., Taylor F., Edwards R. L., and Cabioch G. (1997) Abrupt changes in early Holocene tropical sea surface temperature derived from coral records. *Nature* **385,** 705–707.

Boiseau M. and Juillet-Leclerc A. (1997) H_2O_2 treatment of recent coral aragonite: Oxygen and carbon isotopic implications. *Chem. Geol.* **143,** 171–180.

Busenberg E. and Plummer L. N. (1985) Kinetic and thermodynamic factors controlling the distribution of SO_4^{2-} and Na^+ in calcites and selected aragonites. *Geochim. Cosmochim. Acta* **49,** 713–725.

Delaney M. L., Linn L. J., and Druffel E. R. M. (1993) Seasonal cycles of manganese and cadmium in coral from the Galapagos Islands. *Geochim. Cosmochim. Acta* **57,** 347–354.

Delaney M. L., Linn L. J., and Davis P. J. (1996) Trace and minor element ratios in *Halimeda* aragonite from the Great Barrier Reef. *Coral Reefs* **15,** 181–189.

Dyrssen D. and Wedborg M. (1974) Equilibrium calculations of the speciation of elements in seawater. In *The Sea,* Vol. 5 (ed. E. D. Goldberg), pp. 181–195. Wiley-Interscience.

Enmar R., Stein M., Bar-Matthews M., Sass E., Katz A., and Lazar B. (2000) Diagenesis in live corals from the Gulf of Aqaba. I. The effect on paleo-oceanography tracers. *Geochim. Cosmochim. Acta* **64,** 3123–3132.

Fallon S. J., McCulloch M. T., van Woesik R., and Sinclair D. J. (1999) Corals at their latitudinal limits: Laser ablation trace element systematics in *Porites* from Shirigai Bay, Japan. *Earth Planet. Sci. Lett.* **172,** 221–238.

Gaffey S. J. and Bronnimann C. E. (1993) Effects of bleaching on organic and mineral phases in biogenic carbonates. *J. Sediment. Petrol.* **63,** 752–754.

Gagan M. K., Ayliffe L. K., Hopley D., Cali J. A., Mortimer G. E., Chappell J., McCulloch M. T., and Head M. J. (1998) Temperature and surface-ocean water balance of the mid-Holocene tropical western Pacific. *Science* **279,** 1014–1018.

Gaillardet J. and Allègre C. J. (1995) Boron isotopic compositions of corals; seawater or diagenesis record? *Earth Planet. Sci. Lett.* **136,** 665–676.

Garrels R. M. and Thompson M. E. (1962) A chemical model for sea water at 25°C and one atmosphere total pressure. *Am. J. Sci.* **260,** 57–66.

Goreau T. J. (1977) Coral skeletal chemistry: Physiological and environmental regulation of stable isotopes and trace metals in *Montastrea annularis. Proc. R. Soc. London Ser. B* **196,** 291–315.

Guilderson T. P., Fairbanks R. G., and Rubenstone J. L. (1994) Tropical temperature variations since 20,000 years ago: Modulating interhemispheric climate change. *Science* **263,** 663–665.

Hart S. R., Cohen A. L., and Ramsay P. (1997) Microscale analysis of Sr/Ca and Ba/Ca in *Porites. Proc. 8th Int. Coral Reef Symp. Panama* **2,** 1707–1712.

Hemming N. G. and Hanson G. N. (1992) Boron isotopic composition and concentration in modern marine carbonates. *Geochim. Cosmochim. Acta* **56,** 537–543.

Ishikawa M. and Ichikuni M. (1984) Uptake of sodium and potassium by calcite. *Chem. Geol.* **42,** 137–146.

Kester D. R. and Pytkowicz R. M. (1968) Magnesium sulfate association at 25°C in synthetic seawater. *Limnol. Oceanogr.* **13,** 670–674.

Kester D. R. and Pytkowicz R. M. (1969) Sodium, magnesium and calcium sulfate ion-pairs in seawater at 25°C. *Limnol. Oceanogr.* **14,** 686–692.

Kitano Y., Okumura M., and Idogaki M. (1975) Incorporation of sodium, chloride and sulfate with calcium carbonate. *Geochem. J.* **9,** 75–84.

Land L. S. and Hoops G. K. (1973) Sodium in carbonate sediments and rocks: A possible index to the salinity of diagenetic solutions. *J. Sediment. Petrol.* **43,** 614–617.

Le Tissier M. D'A. A., Clayton B., Brown B. E., and Davis P. S. (1994) Skeletal correlates of coral density banding and an evaluation of radiography as used in sclerochronology. *Mar. Ecol. Prog. Ser.* **110,** 29–44.

Lea D. W., Shen G. T., and Boyle E. A. (1989) Coralline barium records temporal variability in equatorial Pacific upwelling. *Nature* **340,** 373–376.

Linn L. J., Delaney M. L., and Druffel E. R. M. (1990) Trace metals in contemporary and seventeenth-century Galapagos coral: Records of seasonal and annual variations. *Geochim. Cosmochim. Acta* **54,** 387–394.

Love K. M. and Woronow A. (1991) Chemical changes induced in aragonite using treatments for the destruction of organic material. *Chem. Geol.* **93,** 291–301.

McCulloch M., Mortimer G., Esat T., Xianhua L., Pillans B., and Chappell J. (1996) High resolution windows into early Holocene climate: Sr/Ca coral records from the Huon Peninsula. *Earth Planet. Sci. Lett.* **138,** 169–178.

McCulloch M. T., Tudhope A. W., Esat T. M., Mortimer G. E., Chappell J., Pillans B., Chivas A. R., and Omura A. (1999) Coral record of equatorial sea-surface temperatures during the penultimate deglaciation at Huon Peninsula. *Science* **283,** 202–204.

Min G. R., Edwards R. L., Taylor F. W., Recy J., Gallup C. D., and Beck J. W. (1995) Annual cycles of U/Ca in coral skeletons and U/Ca thermometry. *Geochim. Cosmochim. Acta* **59,** 2025–2042.

Mitsuguchi T., Matsumoto E., Abe O., Uchida T., and Isdale P. J. (1996) Mg/Ca thermometry in coral skeletons. *Science* **274,** 961–963.

Mitsuguchi T., Matsumoto E., Abe O., Uchida T., and Isdale P. J. (1997) Magnesium/calcium ratio of coral skeletons as a palaeothermometer. *Proc. 8th Int. Coral Reef Symp. Panama* **2**, 1701–1706.

Oomori T., Kaneshima K., Nakamura Y., and Kitano Y. (1982) Seasonal variation of minor elements in coral skeletons. *Galaxea* **1,** 77–86.

Pingitore N. E., Meitzner G., and Love K. M. (1995) Identification of sulfate in natural carbonates by X-ray absorption spectroscopy. *Geochim. Cosmochim. Acta* **59,** 2477–2483.

Pytkowicz R. M. and Hawley J. E. (1974) Bicarbonate and carbonate ion-pairs and a model of seawater at 25°C. *Limnol. Oceanogr.* **19,** 223–234.

Schneider R. C. and Smith S. V. (1982) Skeletal Sr content and density in *Porites* spp. in relation to environmental factors. *Mar. Biol.* **66,** 121–131.

Shannon R. D. (1976) Revised effective ionic and systematic studies of interatomic distances in Halides and Chalocogenides. *Acta Crystallogr.* **A32**, 751–767.

Shen G. T. and Boyle E. A. (1987) Lead in corals: Reconstruction of historical industrial fluxes to the surface ocean. *Earth Planet. Sci. Lett.* **82,** 289–304.

Shen G. T., Boyle E. A., and Lea D. W. (1987) Cadmium in corals as a tracer of historical upwelling and industrial fallout. *Nature* **328,** 794–796.

Shen G. T. and Boyle E. A. (1988) Determination of lead, cadmium and other trace metals in annually-banded corals. *Chem. Geol.* **67,** 47–62.

Shen G. T. and Dunbar R. B. (1995) Environmental controls on uranium in reef corals. *Geochim. Cosmochim. Acta* **59,** 2009–2024.

Shen G. T. and Sanford C. L. (1990) Trace element indicators of climate variability in reef-building corals. In *Global Ecological Consequences of the 1982–83 El Niño–Southern Oscillation* (ed. P. W. Glynn), pp. 255–283. Elsevier.

Shen G. T., Campbell T. M., Dunbar R. B., Wellington G. M., Colgan M. W., and Glynn P. W. (1991) Paleochemistry of manganese in corals from Galapagos Islands. *Coral Reefs* **10,** 91–100.

Shen G. T., Cole J. E., Lea D. W., Linn L. J., McConnaughey T. A., and Fairbanks R. G. (1992a) Surface ocean variability at Galapagos from 1936–1982: Calibration of geochemical tracers in corals. *Paleoceanography* **7,** 563–588.

Shen G. T., Linn L. J., Campbell T. M., Cole J. E., and Fairbanks R. G. (1992b) A chemical indicator of trade wind reversal in corals from the western tropical Pacific. *J. Geophys. Res.* **97,** 12689–12697.

Sinclair D. J., Kinsley L. P. J., and McCulloch M. T. (1998) High resolution analysis of trace elements in corals by laser ablation ICP-MS. *Geochim. Cosmochim. Acta* **62,** 1889–1901.

Smith S. V., Buddemeier R. W., Redalje R. C., and Houck J. E. (1979) Strontium-calcium thermometry in coral skeletons. *Science* **204,** 404–406.

Swart P. K. and Hubbard J. A. E. B. (1982) Uranium in scleractinian coral skeletons. *Coral Reefs* **1,** 13–19.

Uchida T., Kojima I., and Iida C. (1980) Determination of metals in small samples by atomic absorption and emission spectrometry with discrete nebulization. *Anal. Chim. Acta* **116,** 205–210.

Vengosh A., Kolodny Y., Starinsky A., Chivas A. R., and McCulloch M. T. (1991) Coprecipitation and isotopic fractionation of boron in modern biogenic carbonates. *Geochim. Cosmochim. Acta* **55,** 2901–2910.

Wainwright S. A. (1964) Studies of the mineral phase of coral skeleton. *Exp. Cell Res.* **34,** 213–230.

Walls R. A., Ragland P. C., and Crisp E. L. (1977) Experimental and natural early diagenetic mobility of Sr and Mg in biogenic carbonates. *Geochim. Cosmochim. Acta* **41,** 1731–1737.

Weber J. N. (1973) Incorporation of strontium into reef coral skeletal carbonate. *Geochim. Cosmochim. Acta* **37,** 2173–2190.

White A. F. (1977) Sodium and potassium coprecipitation in aragonite. *Geochim. Cosmochim. Acta* **41,** 613–625.

Yoshioka S., Ohde S., Oomori T., and Kitano Y. (1985) Dissolution of magnesium and strontium during the transformation of coral aragonite to calcite in aqueous solution. *Galaxea* **4,** 99–111.